

Hydroacoustic Absorption and Amplification by Turbulence

Kai-Xin Hu^{a,b,1}, Yue-Jin Hu^c

^aZhejiang Provincial Engineering Research Center for the Safety of Pressure Vessel and Pipeline, Ningbo University, Ningbo, Zhejiang 315211, China

^bKey Laboratory of Impact and Safety Engineering (Ningbo University), Ministry of Education, Ningbo, Zhejiang 315211, China

^cNingbo Jiangbei District People's Government, Ningbo, Zhejiang, 315800, China

Abstract

Acoustic waves propagating through fluid media are significantly influenced by turbulence. This paper experimentally investigates the influence of underwater turbulence on the propagation characteristics of acoustic waves, revealing that acoustic waves can be absorbed or amplified at frequencies far exceeding the turbulent fluctuation frequency. The maximum observed attenuation or amplification of received signals exceeds 60%, with no spectral broadening. The study covers two flow conditions: pipe flow and free jet, driven by either a pump or hydraulic head difference. Hydroacoustic transducers with frequencies ranging from 60 kHz to 4.4 MHz are used, while the wave propagation directions both parallel and perpendicular to the mean flow are considered. The variation trend and magnitude of received signals depend on wave frequency, amplitude and flow conditions. For each case, the amplitudes of all frequency components simultaneously decreases or increases under

¹Corresponding author, Email: hukaixin@nbu.edu.cn

turbulence, with no new spectral components appearing. After closing the flow control valve, the receiver signal requires a finite time to stabilize to its quiescent-state value. In contrast, suction near the pipe outlet shows that laminar flow has no effect on acoustic signals, confirming that the primary cause of signal variation is turbulent fluctuations rather than mean flow. Comparison with conventional theories and experiments indicates that mechanisms such as bubbles, resonance, scattering, or viscous dissipation cannot explain the observed phenomena. This suggests the existence of a previously unknown interaction mechanism between turbulence and acoustic waves.

1. Introduction

When acoustic waves propagate through a fluid medium, their amplitude, frequency, and direction of propagation can be altered by turbulence. This phenomenon is of great significance for understanding the laws of acoustic wave propagation and the characteristics of turbulent motion, making the interaction between acoustic waves and turbulence a subject of enduring research interest.

The earliest studies on this topic trace back to Lighthill [1] in his pioneering work on aerodynamic sound. This issue represents not only a fundamental theoretical challenge in fluid dynamics but also holds substantial applied value in fields such as aircraft noise and hydroacoustics. Consequently, subsequent research has yielded significant theoretical and experimental progress in related areas.

First, acoustic waves can be scattered by turbulence. When a sound wave passes

through a turbulent region with concentrated vorticity, spatial inhomogeneities in sound speed cause wave scattering. This problem was first independently studied by Lighthill [2] and Kraichnan [3], and later extended by multiple researchers [4,5]. A key characteristic of sound wave scattering by turbulence is the spectral broadening. Campos [6,7] conducted a theoretical study on the spectral broadening of sound wave through turbulent shear layers and compared it with the experimental results relevant to the study of aircraft noise. Korman & Beyer [8,9] experimentally examined the scattering of sound by turbulence in water, confirming the characteristics of spectral broadening. In this experiment, a single monochromatic sound wave is scattered in a confined region of turbulence which is created by a submerged water jet.

Second, turbulence can absorb acoustic waves. In studies of sound scattering by turbulence, researchers typically assume that turbulence remains unaffected by the acoustic wave, with sound energy merely being redistributed in all directions. This assumption holds only when the characteristic frequencies of turbulence and sound waves differ significantly. When this condition is not met, a substantial portion of acoustic energy may be absorbed by turbulence.

Ingard & Singhal [10] experimentally investigated acoustic attenuation in turbulent gas flows within pipes, attributing the damping to viscous dissipation and thermal conduction near pipe walls. Howe [11] theoretically analyzed sound attenuation through turbulent regions, comparing the attenuation coefficient with experimental data from Ronneberger & Ahrens [12]. He concluded that this attenuation arises from strain generated by the acoustic field, with strain magnitudes sharply increasing near

solid boundaries. Maximum attenuation occurs when acoustic and turbulent time scales are comparable. Peters et al. [13] measured the damping and reflection coefficients of plane acoustic waves in smooth pipes (gaseous medium), confirming Ronneberger & Ahrens' [12] findings. Weng, Boij & Hanifi [14,15] conducted theoretical and numerical studies on acoustic attenuation in pipe turbulence, validating results against prior experiments [12,13].

From the aforementioned studies, it can be observed that experimental research on the interaction between turbulence and acoustic waves has historically focused primarily on aeroacoustics, with limited exploration in hydroacoustics. To our knowledge, the only relevant experiments are those by Ronneberger & Ahrens [12] on pipe turbulence and Korman & Beyer [8,9] on submerged jet turbulence. The observed phenomena of acoustic wave absorption and scattering by turbulence largely align with classical theories. However, these experiments are outdated and limited in scope, failing to fully reveal the underlying mechanisms of hydroacoustic wave propagation in turbulent flows.

In this study, we employ transducers to analyze the characteristics of hydroacoustic waves after interaction with turbulence. Our results demonstrate that acoustic waves can be absorbed or amplified by turbulence, with no observed spectral broadening. These findings, particularly within the tested parameter ranges, cannot be fully explained by conventional theories, suggesting the existence of previously unknown mechanisms governing turbulence-acoustic interactions.

This paper is organized as follows. First, we present the experimental setup, which

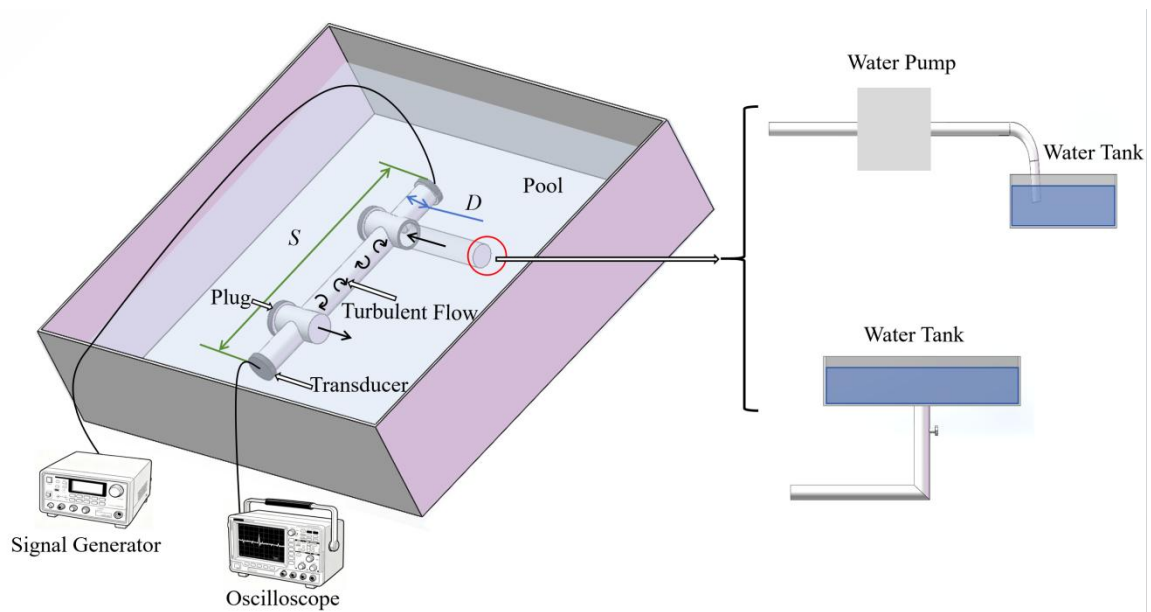
includes two configurations: a pipe flow and a submerged water jet. The flows are driven by a high-pressure pump and hydraulic head difference respectively, with acoustic waves propagating either parallel or perpendicular to the mean flow direction. Subsequently, we present the experimental results obtained under various flow conditions. Following this, we conduct a comparative analysis with previous studies, systematically examining potential explanations for the observed signal variations within the framework of classical theories before rejecting them one by one. Finally, we summarize the key conclusions of this study.

2. Experimental Setup

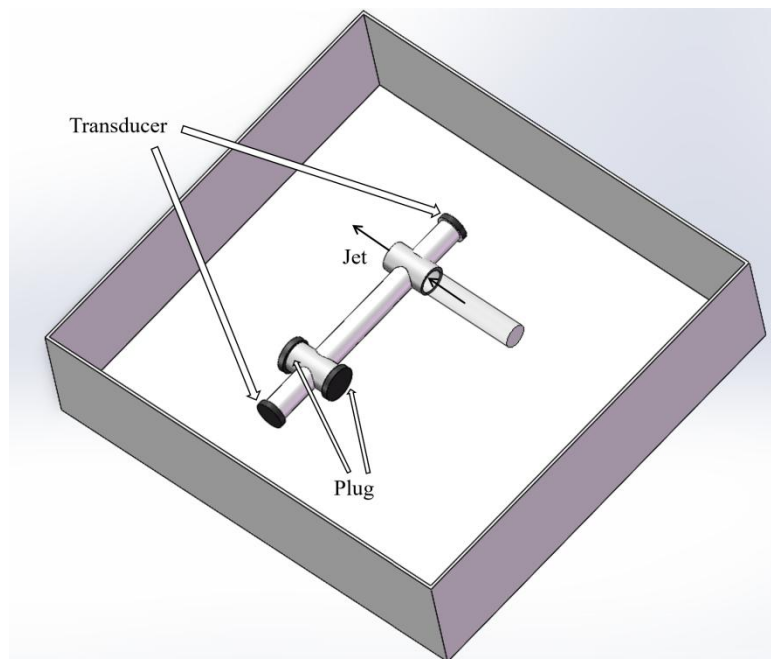
The submerged experimental setup comprises two primary configurations: (1) pipe flow (Figure 2.1), which includes both parallel (sub-divided into co-directional and counter-directional cases) and perpendicular propagation relative to the mean flow direction, and (2) free jet flow (Figure 2.2). This systematic design allows for comprehensive investigation of flow-acoustic interaction mechanisms, particularly in examining direction-dependent wave modulation effects, where the parallel/perpendicular configurations effectively isolate axial versus transverse interaction components.

In Figure 2.1(a), two hydroacoustic transducers mounted at opposite ends of the pipeline are connected to a signal generator and an oscilloscope, serving as the acoustic emitter and receiver, respectively. During experiments, the signal generator emits single-frequency sinusoidal waves. Due to the high operating frequency, the received signal spectrum displayed on the oscilloscope exhibits measurable

bandwidth (Figures 3.3, 3.4). External water flow enters through the pipeline inlet and exits at the outlet. Acoustic waves propagating axially along the pipe are subject to turbulence modulation. The signal generator controls the incident acoustic wave, while the oscilloscope measures received signals under both static and flowing conditions, including amplitude variations across frequencies.



(a)



(b)

Figure 2.1 Schematic diagram of the experimental setup for acoustic wave-turbulence interaction in pipe flow, showing the relative directions of acoustic propagation and mean flow: (a) parallel; (b) perpendicular.

For the free jet configuration (Figure 2.2a), pressurized water from the pump exits through the nozzle into the pool, forming a free jet. Acoustic emitter and receiver are positioned on opposite sides of the jet, with the acoustic propagation direction perpendicular to the mean flow direction. In Figure 2.2(b), the receiver can be rotated to measure received signals at different angular positions. Detailed parameters for both Figures 2.1 and 2.2 are provided in Appendix Table 4.

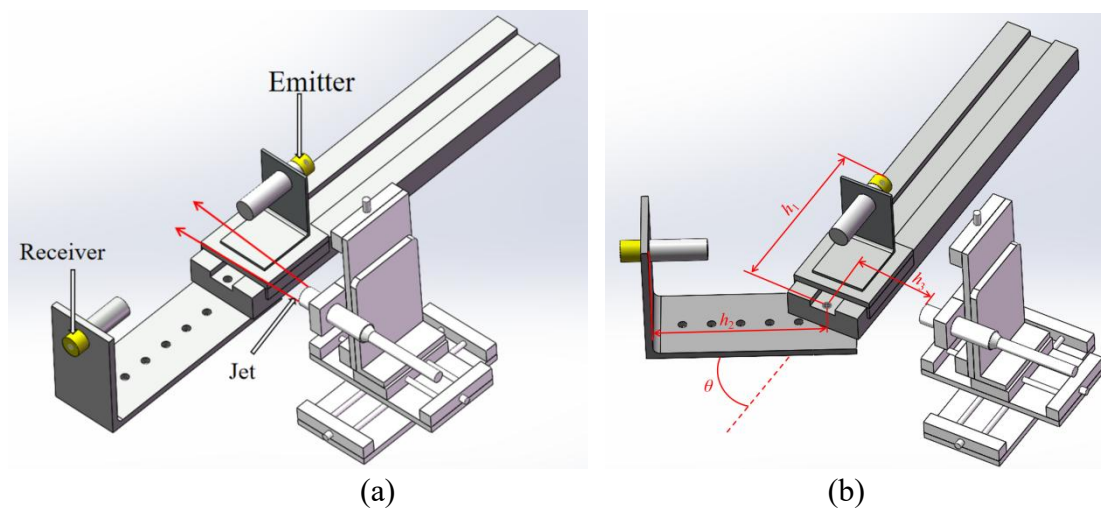


Figure 2.2 Schematic diagram of the experimental setup for acoustic wave-turbulence interaction in a free jet flow, showing configurations of : (a)collinear alignment – emitter and receiver axes coincide vertically with the mean flow direction; (b) angular offset – receiver axis inclined at the angle θ relative to the emitter.



(a)



(b)

Figure 2.3 Flow driving systems: (a) Pump-driven; (b) Tank-pipeline system.

The water flow is driven by two methods: a high-pressure pump and hydraulic head difference (HHD). Figure 2.3 shows actual photographs of the experimental setup. For the pump configuration, a flowmeter is installed in the inlet pipeline, with a stabilized flow rate of (7.2 ± 0.1) L/min during operation. For the HHD case (Figure 2.3b), the

height difference between the water tank surface and the pool surface is maintained at $(1.85 \pm 0.05)\text{m}$ during experiments.

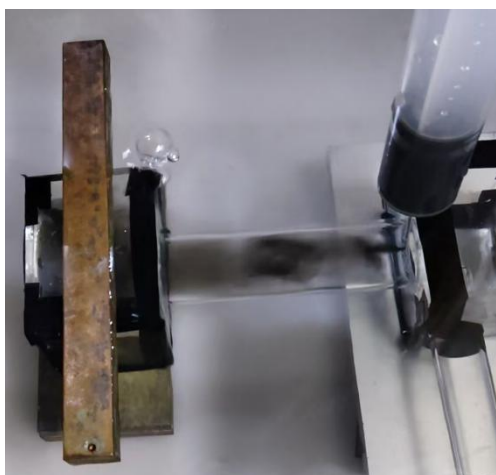
3. Results

3.1 Pipe flow

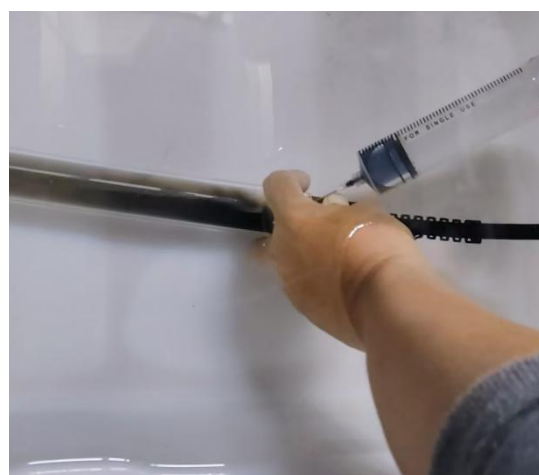
First, we examine the flow state, then discuss the cases when acoustic waves propagate either parallel or perpendicular to the mean flow direction, respectively.

3.1.1 Examine flow state

To examine flow states, dye is injected into the pipe. Figure 3.1 compares three scenarios: (1) flow driven by HHD (Video 1), (2) pump-driven jet flow (Video 2), and (3) pump suction flow (Video 3). In the first two cases, the dye rapidly filled the entire pipe, confirming fully developed turbulent flow due to valve-induced disturbances and prolonged wall friction in long pipelines. In contrast, the third case exhibited clear, stable dye streamlines, indicating laminar flow—a result of a lower flow rate inside the pipe.



(a)



(b)

1	HHD	Same	1	18.7	0.9	10	21.2±0.2	35.7±1.48	↑,68.4%
2	HHD	Same	1	18.9	1.0	1	23.8±0.2	17.2±0.64	↓,27.7%
3	HHD	Opposite	1	19.0	0.9	10	26.8±0.2	38.5±0.36	↑,43.7%
4	HHD	Opposite	1	19.0	1.0	1	24.4±0.2	17.9±0.40	↓,26.7%
5	HHD	Same	1	17.8	1.3	15	20.6±0.2	17.0±0.25	↓,17.5%
6	Pump	Same	1	18.1	1.0	1	21.2±0.2	16.0±0.20	↓,24.5%
7	Pump	Same	0.2	17.9	0.2	0.5	64.3±0.4	14.7±0.30	↓,77.1%
8	Pump	Perpendicular	0.2	17.9	0.2	0.5	29.0±0.2	21.1±0.31	↓,27.1%
9	Pump	Same	0.2	17.2	0.06	20	12.5±0.12	10.4±0.28	↓,16.8%
10	HHD	Same	2	17.9	2	10	23.6±0.2	22.0±0.24	↓,6.8%
11	HHD	Same	4	18.1	4	10	25.2±0.2	28.3±1.05	↑,12.3%
12	HHD	Same	4	18.1	4.4	10	23.6±0.2	26.0±3.90	↑,10.2%
13	HHD	Perpendicular	1	17.6	0.9	10	22.3±0.2	26.1±0.21	↑,17.0%
14	HHD	Perpendicular	1	17.6	1.3	15	25.0±0.2	22.7±0.33	↓,9.2%

3.1.2 Parallel

First, we conduct pipe flow experiments using 1 MHz transducers as both acoustic emitter and receiver, with flow driven by HHD (Figure 3.2). Under static conditions (0.9MHz emission at 10.0V), the receiver amplitude is $V_2=21.2\text{mv}$. The acoustic wave propagates in the same direction as the mean flow. When turbulent flow is initiated, the average amplitude increased by 68.4% to $V_3=35.7\text{mv}$ (Video 4, Table 1 Line 1). When emission is stopped, receiver amplitude dropped to 0 mV immediately,

confirming that the incident wave is amplified by the turbulence, while turbulence alone cannot generate acoustic waves at this frequency. Frequency analysis reveals: (1) consistent peak amplitude at 900.01kHz (vs. 900.11kHz minimum, Figure 3.3), (2) synchronous amplitude variations across all frequencies, and (3) no spectral broadening within the oscilloscope's 1Hz resolution - demonstrating perfect frequency preservation between emitted and received signals. These findings validate that turbulent flow under these conditions amplifies incident acoustic waves without inducing frequency shifts.

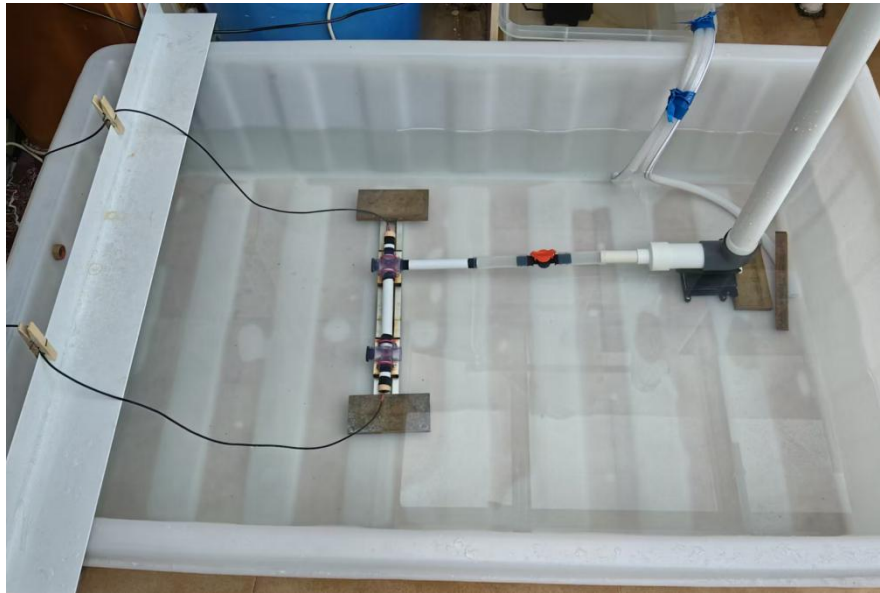
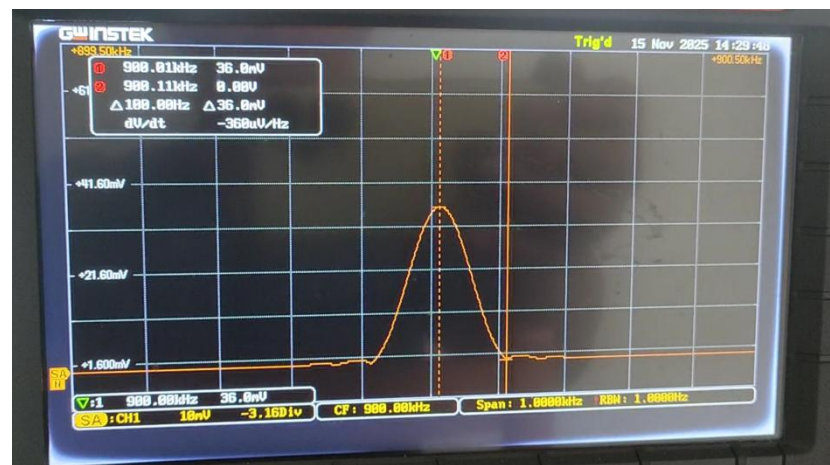


Figure 3.2 Experimental setup of acoustic-turbulence interaction in a pipe flow driven by hydraulic head difference.



(a)

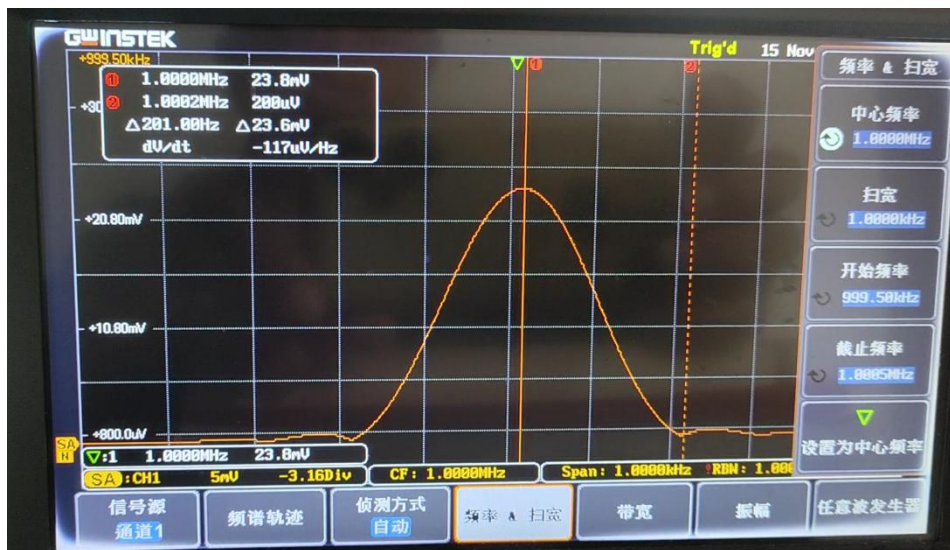


(b)

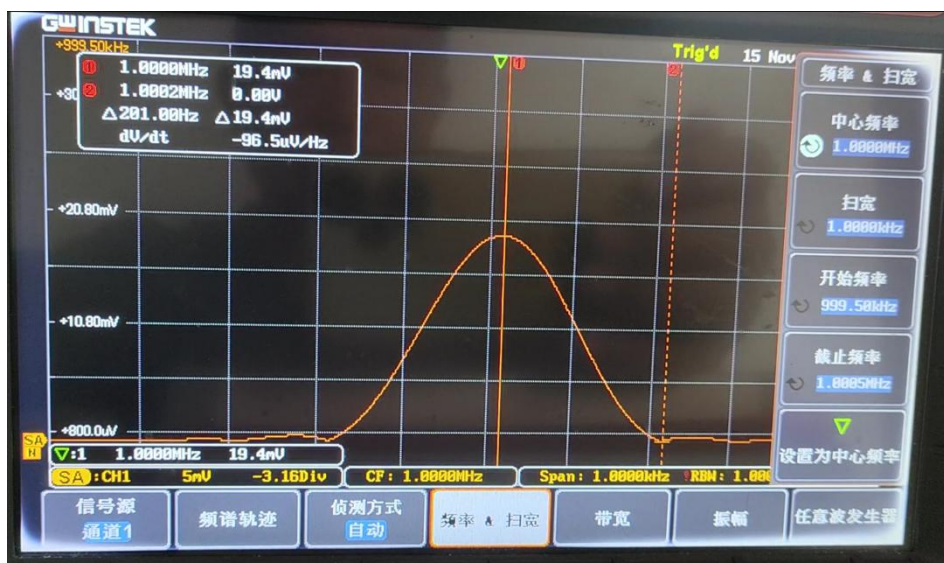
Figure 3.3 Acoustic wave spectrum at 0.9MHz in a pipe flow: (a) static state; (b) turbulent flow.

We configure the acoustic emitter to emit a 1.0 MHz signal at 1.0V (Video 5, Table 1 Line 2). The receiver amplitude decreases from $V_2=23.8$ mV (static water) to an average $V_3=17.2$ mV (turbulent flow), representing a 27.7% reduction. Signal termination tests confirmed immediate amplitude drop to zero upon emitter deactivation, proving this attenuation results exclusively from turbulence absorption of incident waves. Spectral analysis (Figure 3.4) shows no spectral broadening.

Combined with prior 0.9 MHz experiments, these results conclusively demonstrate frequency-dependent acoustic modulation in pipe flows.



(a)



(b)

Figure 3.4 Acoustic wave spectrum at 1.0 MHz in a pipe flow: (a) Static state; (b) Turbulent flow.

Our experimental observations reveal a significant delay in signal recovery after valve closure, with the receiver taking an extended period to stabilize at the original

static value V_2 . This phenomenon occurs because while the valve closure immediately reduces mean flow velocity to zero, turbulent fluctuations within the pipe persist due to fluid inertia. These residual turbulent motions gradually dissipate through viscous damping, during which the receiver signal exhibits decay before ultimately returning to its baseline level.

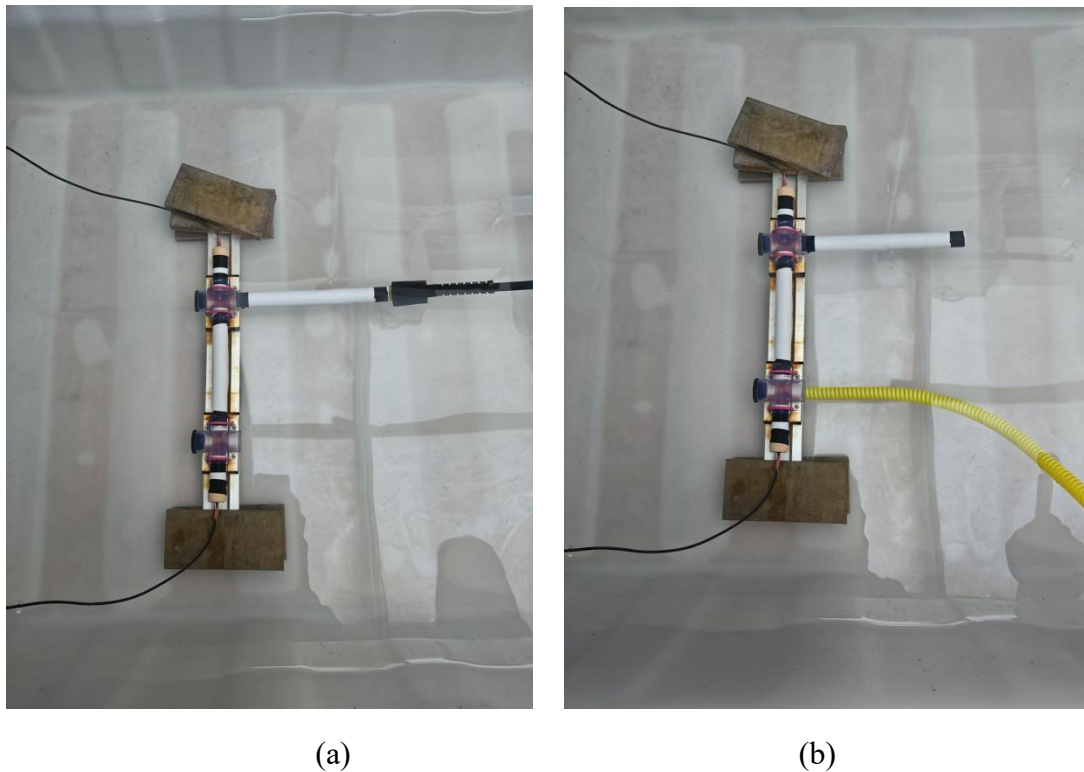


Figure 3.5 Experimental setup of acoustic-turbulence interaction in a pipe flow driven by a pump : (a) Inject at the inlet; (b) Suction at the outlet. The fundamental frequency of the transducer is 1 MHz.

To verify this phenomenon, we inject turbulent flow into the pipe inlet using a pump nozzle (Figure 3.5, Line 6 in Table 1). The frequency of acoustic wave is 1.0MHz. When the received signal changes ($V_3= 16.0$ mV), we immediately remove the nozzle (Video 6). Notably, the signal does not immediately recover to its static

value ($V_2=21.2$ mV). Subsequently, we apply suction near the pipe outlet using the pump's intake. This intervention causes the received signal to rapidly return to V_2 . The restoration occurs because suction changes the internal flow into laminar regime, eliminating turbulent fluctuations and thus recovering the acoustic amplitude. The differential recovery behavior under identical flow parameters proves that: acoustic amplitude variation depends on turbulence intensity; laminar flow conditions permit complete signal restoration; mean flow alone cannot explain observed signal changes.

For the case with a transmitted signal frequency of 1.3 MHz, input voltage $V_1 = 15\text{V}$ (Line 5 in Table 1), the received acoustic wave amplitude decreased from $V_2 = 20.6$ mV (static water) to $V_3 = 17.0$ mV under turbulent flow—a reduction of 17.5%.

When we reverse the wiring connections of the two hydroacoustic transducers to make the acoustic waves propagate against the water flow—transmitting 0.9 MHz and 1.0 MHz signals respectively, we observe that the trend of acoustic amplitude variation remains consistent with the co-directional (forward) propagation case. However, the magnitude of the changes differs (see Lines 3 and 4 in Table 1).

In addition, we have also observed that the same acoustic signal can be either reduced or amplified under the influence of turbulence with different intensities. When the input voltage of the transmitter is $V_1=2\text{V}$, the frequency is 0.9 MHz, the water temperature is 14.5°C , turbulence is injected by a water pump, and the acoustic wave moves in the same direction as the water flow (Fig. 3.5a, Video 7), the acoustic amplitude of the receiver is $V_2=4.24\text{mV}$ when the water is stationary. After the water pump is started, the amplitude rises within a short period of time and then rapidly

drops to a stable value of $V_3=2.64\text{mv}$. After the water pump is turned off, the received signal gradually rises until it reaches the maximum value $V_4=9.35\text{mv}$, then gradually decreases, and takes a long time to return to the initial stationary value. The above phenomenon indicates that the turbulence maintained by water injection from the water pump reduces the acoustic amplitude, while the gradually decaying turbulence in the pipeline after the pump is turned off instead amplifies the acoustic amplitude.

We investigate the influence of the transmitted signal amplitude on the receiver's output amplitude. Figure 3.6 displays the voltage values of the received signal V_r under different voltages of the transmitted signal V_1 . Here, V_r includes V_2 , V_3 , and V_4 , which respectively correspond to the received signal voltage under static water, the stable value after the water pump is started, and the maximum value achievable after the water pump is turned off. The standard deviation in the figure is very small, so most error bars are not displayed. It can be seen that V_2 , V_3 , and V_4 are all approximately proportional to V_1 ; that is, under small input voltages, the reduction and amplification ratios of the received signal are independent of the input voltage V_1 . Therefore, we can conclude that when the input voltage approaches 0 (i.e., the acoustic amplitude is infinitely small), the phenomena of acoustic waves being absorbed and amplified by turbulence will still exist.

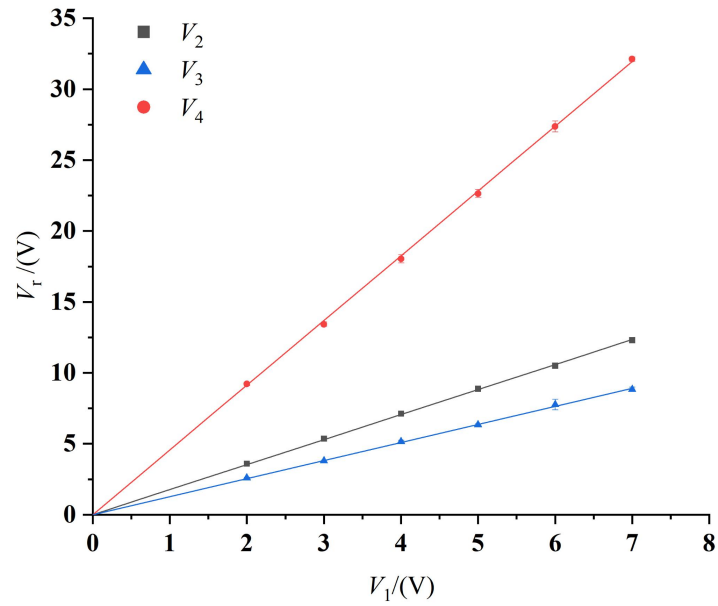


Figure 3.6 The voltage values of the received signal V_r under different voltages of the transmitted signal V_1 . Among them, V_r includes V_2 , V_3 , and V_4 , which respectively correspond to the received signal voltage under static water, the stable value after the water pump is started, and the maximum value achievable after the water pump is turned off. The frequency of the transmitted signal is 0.9 MHz, the water temperature is 14.5°C, turbulence is injected by a water pump, and the sound wave moves in the same direction as the mean flow.

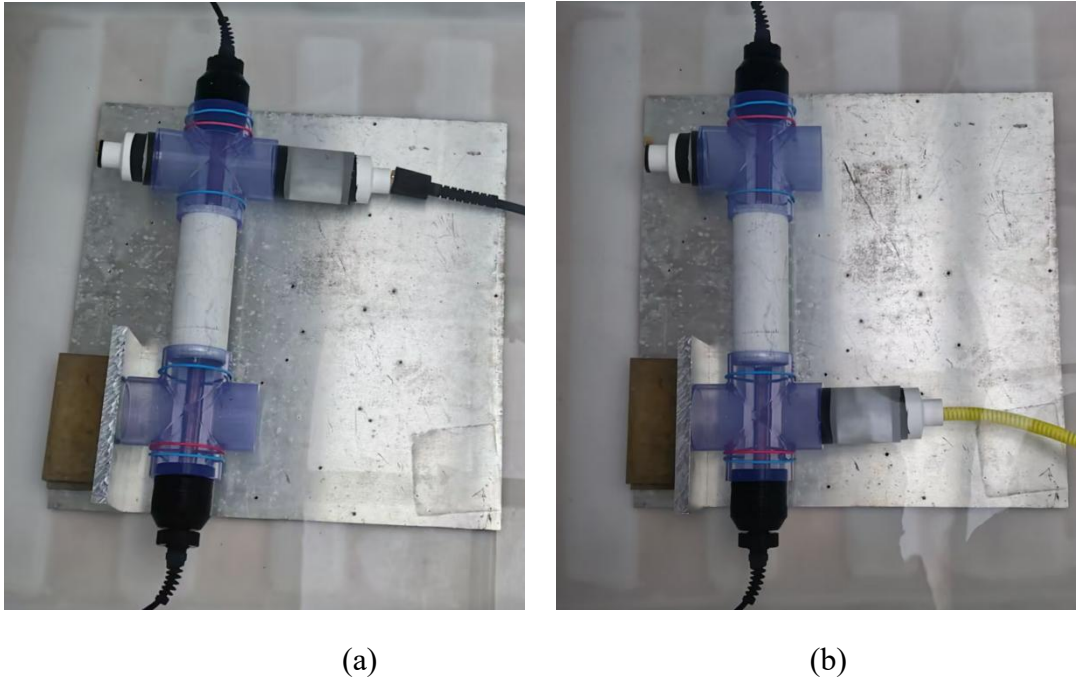


Figure 3.7 Experimental setup of acoustic-turbulence interaction in a pipe flow driven by a pump: (a) inject at the inlet; (b) suction at the outlet. The fundamental frequency of the transducer is 200KHz.

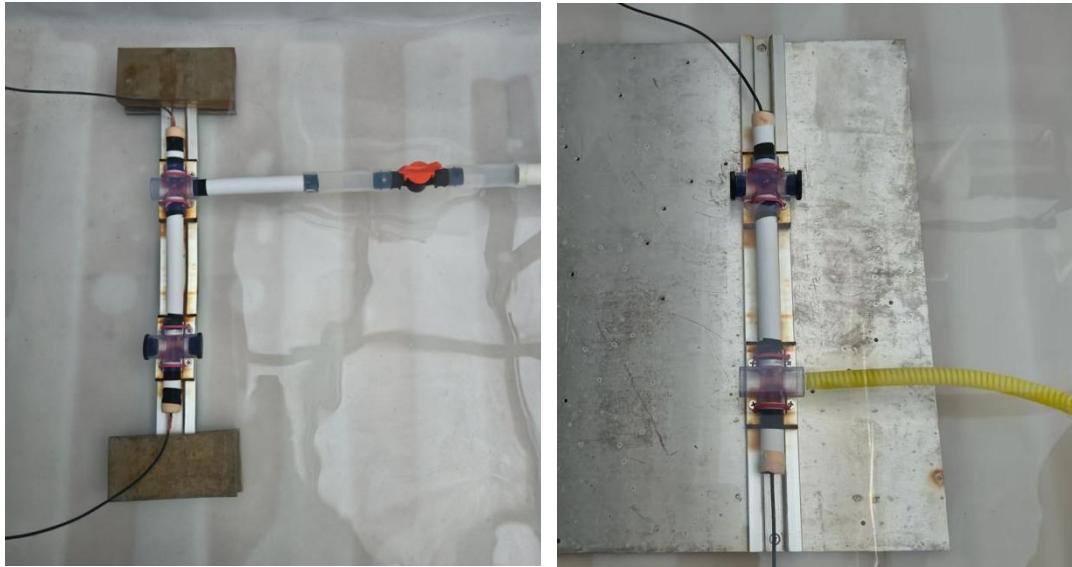
In the experiment of Figure 3.7, 200 kHz transducers serve as both the acoustic emitter and receiver. The transmitted signal is set to 200 kHz at an excitation voltage of $V_1 = 0.5$ V while water is injected into the pipeline using a pump (Line 7, Table 1). When the acoustic wave propagates co-directionally with the flow, the received signal voltages measure $V_2=64.3\text{mV}$ (Static) and $V_3=14.8\text{mV}$ (Turbulent), demonstrating a 77.1% attenuation. No signal is detected when the transmitter is deactivated, and spectral analysis confirms no spectral broadening. Notably, when suction is applied near the pipeline outlet, the received signal voltage (63.2 mV) matches the static flow condition (Video 8), conclusively proving that laminar flow induces no acoustic modulation. This confirms that turbulent fluctuations—rather than mean flow—are

the primary mechanism for signal attenuation. In a complementary test at 60 kHz with $V_1 = 20$ V (Line 7, Table 1), the observed voltages $V_2 = 12.5$ mV and $V_3 = 10.4$ mV corresponds to a 16.8% reduction, further validating the frequency-dependent attenuation characteristics.

At 2 MHz and 4 MHz, we observe both amplitude decreases and increases in received signals under turbulent flow conditions (Lines 10-11, Table 1). The most remarkable behavior occurs at 4.4 MHz, where turbulent flow induces significant signal oscillations. While the time-averaged amplitude shows an increase, yet instantaneous measurements repeatedly drop below the static value (Video 9). These results clearly show that turbulence simultaneously produces two competing effects: acoustic energy absorption (manifested as signal attenuation) and amplification (seen as signal enhancement), with the dominant effect depending on instantaneous flow structure.

3.1.2 Perpendicular

When the acoustic waves propagate perpendicular to the mean flow, we conduct experiments with different frequencies and driving methods (Lines 8, 13, 14 in Table 1). The results show that no spectral broadening occurs in this configuration. The trend of amplitude variation remains similar to the parallel case, but the magnitude of change is significantly smaller. The reason can be explained as follows: when waves propagate parallel to the mean flow, their interaction with turbulence occurs over a longer axial distance (compared to perpendicular case), leading to more pronounced variations. Suction near the pipe opening does not alter the received signal.



(a)

(b)

Figure 3.8 Experimental setup for acoustic waves propagate perpendicular to the mean flow: (a) inject at the inlet driven by hydraulic head difference; (b) suction at the outlet driven by a pump. The fundamental frequency of the transducer is 1MHz.

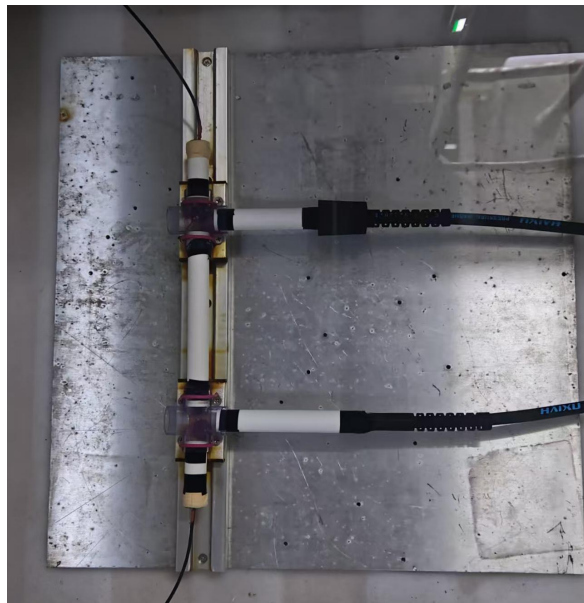


Figure 3.9 Experimental setup of acoustic waves propagate perpendicular to the mean flow with two water inlets. Here, the two inlets are supplied with water flow by two water pumps, respectively. The fundamental frequency of the transducer is 1 MHz.

From the previous experiments, we hypothesize that during the process of acoustic waves being absorbed and amplified by turbulence, the total effect of acoustic wave absorption (amplification) by the turbulence in the entire pipeline should be equal to the product of the effects of acoustic wave absorption (amplification) by the turbulence in each segment of the pipe. To verify this hypothesis, we conduct the following experiment (Fig. 3.9): two water inlets are installed in the pipeline, and water flow is injected through each inlet by two separate water pumps, resulting in the acoustic waves being perpendicular to the mean flow. This setup creates two regions with concentrated turbulence in the pipeline, and the two regions are approximately independent of each other.

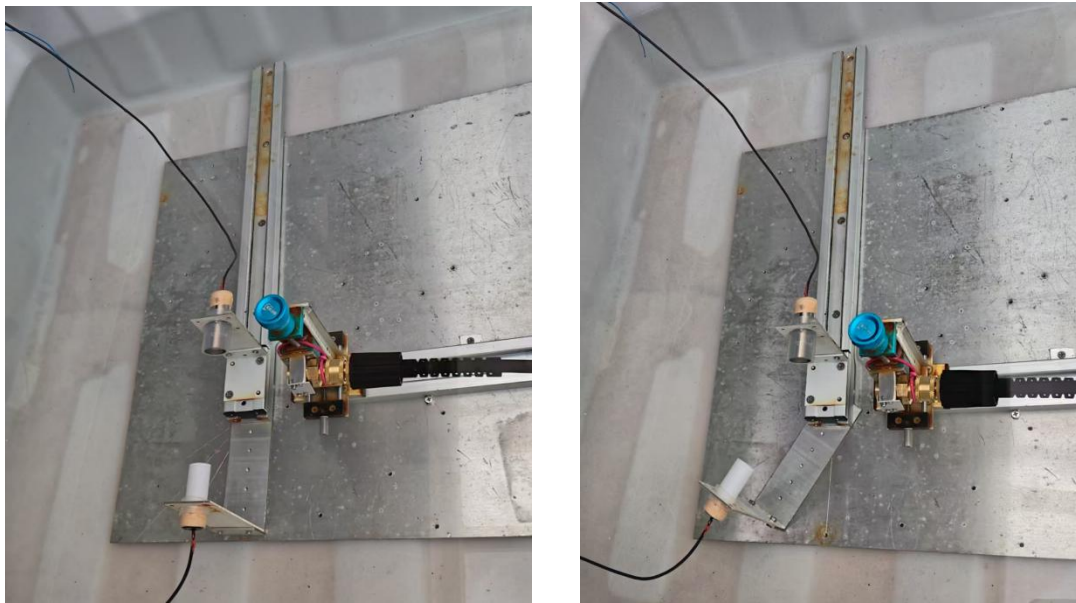
Table 2 shows the received signal values when the two water pumps are activated separately and jointly. Among them, $V_{r1}(V_{r2})$ represents the amplitude of the received signal when a single water pump is activated to inject water into the inlet close to the transmitting end (receiving end). V_{r12} denotes the amplitude of the received signal when both water pumps are activated simultaneously. The amplification factors of the acoustic signal when the two water pumps are independently activated are $V_{r1}/V_2, V_{r2}/V_2$, respectively. The theoretical total amplification factor when both water pumps are activated simultaneously is the product of the amplification factors when they are independently activated, i.e., $(V_{r1} \cdot V_{r2})/V_2^2$, while the actual measured value is V_{r12}/V_2 . It can be observed that the theoretical value is very close to the actual measured value.

Table 2 Amplitude of acoustic waves in pipelines with two water inlets under various conditions.

No.	Temperature (°C)	Emitter			Receiver			Theoretical total amplification factor	Actual total amplification factor
		Frequency (MHz)	Voltage V_1 (V)	Static V_2 (mV)	V_{r1} (mV)	V_{r2} (mV)	V_{r12} (mV)		
1	16.1	0.9	5	12.5±0.1	9.84±0.06	10.0±0.04	7.84±0.04	$\frac{V_{r1} \cdot V_{r2}}{V_2^2}$	$\frac{V_{r12}}{V_2}$
								63.0%	62.7%
2	16.5	1.0	1	16.2±0.1	17.4±0.1	17.8±0.1	19.2±0.1		
								118.0%	118.5%
3	15.8	1.1	0.5	10.0±0.04	9.36±0.04	9.60±0.04	8.72±0.04		
								89.8%	87.2%
4	16.5	1.2	1.5	14.6±0.1	12.6±0.1	12.2±0.1	10.8±0.04		
								72.1%	74.0%

3.2 Free Jet

For the free jet configuration, we position the emitter and receiver on opposite sides of the jet (Figure 3.10), with the receiver being rotatable. First examining the case where the azimuth angle $\theta=0^\circ$ (acoustic waves propagate perpendicular to the mean flow), for 0.9MHz and 1.0MHz waves (Lines 1,2 in Table 3), with jet turbulence present, the received signals show distinct increases and decreases respectively compared to static state. The amplitude variations are smaller than those observed in pipe flow conditions. No Doppler shift or spectral broadening are detected. For 1.3MHz waves (Line 3 in Table 3), turbulent flow causes significant oscillations in the received signal, while the time-averaged signal amplitude shows small change compared to stationary conditions.



(a)

(b)

Figure 3.10 Experimental setup of acoustic wave interaction with free jet flow: (a) $\theta=0^\circ$; (b) $\theta=30^\circ$. The fundamental frequency of the transducer is 1 MHz.

We subsequently measure received signals at various azimuth angles (Lines 4-11 in Table 3). The experimental data reveal signal attenuation: rapid signal degradation occurs when $\theta \geq 15^\circ$. Negligible amplitude variation is observed before/after jet initiation. The measurement resolution is 0.08mV. Similar attenuation patterns are observed for $\theta < 0^\circ$. These findings confirms the absence of significant turbulent scattering to other angular directions.

Table 3 Acoustic signals in free jet under various conditions.

No.	Drive Mode	azimuth angle θ ($^\circ$)	TFF (MHz)	Temperature ($^\circ\text{C}$)	Emitter		Receiver		
					Frequency (MHz)	Voltage V_1 (V)	Static V_2 (mV)	Turbulence V_3 (mV)	The relative change V_a
1	Pump	0	1	16.1	0.9	9	12.8 \pm 0.1	13.6 \pm 0.14	\uparrow ,6.3%
2	Pump	0	1	16.0	1.2	2	14.1 \pm 0.1	12.7 \pm 0.31	\downarrow ,9.9%
3	Pump	0	1	16.1	1.3	7	11.8 \pm 0.1	11.9 \pm 0.41	—
4	Pump	15	1	16.1	0.9	9	0.48~0.56	0.48~0.56	—
5	Pump	30	1	16.1	0.9	9	0.16	0.16	—
6	Pump	45	1	16.1	0.9	9	0.16	0.16	—
7	Pump	60	1	16.1	0.9	9	0.16	0.16	—
8	Pump	15	1	16.0	1.2	2	0.40 \pm 0.08	0.40 \pm 0.08	—
9	Pump	30	1	16.0	1.2	2	0.08	0.08	—
10	Pump	45	1	16.0	1.2	2	0~0.08	0~0.08	—

4. Discussion

Below, we attempt to identify the causes of acoustic variations under turbulent conditions from conventional theories, systematically eliminating potential explanations while conducting comparative analysis with previous literature. Sections 4.1-4.5 examine pipe flow conditions, while Section 4.6 investigates jet flow conditions.

4.1 Bubble

Experimental results demonstrate that when the pipe is submerged in water, residual air bubbles inside the pipe can significantly affect the amplitude of acoustic waves received by the transducer. This suggests that the presence of bubbles in flowing water within the pipe may similarly interfere with acoustic signals.

For instance, when a nozzle with diameter $D_1=1\text{mm}$ is attached to the inlet (Figure 4.1a, Video 10), visible bubbles are observed in the ejected water stream. These bubbles caused a drastic reduction in received signal amplitude. This phenomenon is attributed to cavitation induced by excessive flow velocity at the nozzle, which masks the underlying turbulence-acoustic interaction mechanisms.

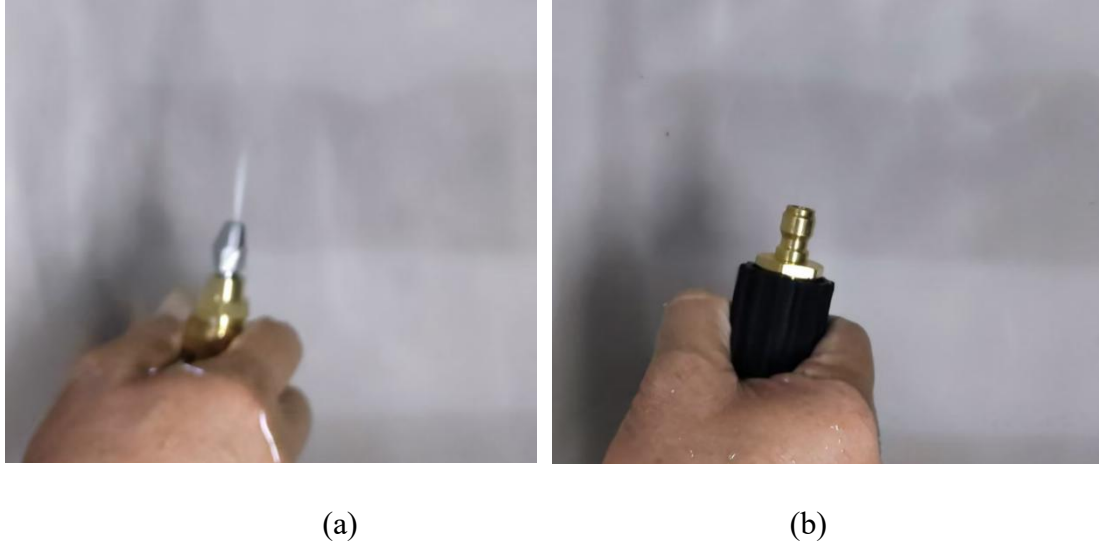


Figure 4.1 Pump-driven jet with the nozzle diameter: (a)1mm;(b)7mm.

When the nozzle diameter is $D_0=7\text{mm}$, no visible bubbles are observed (Fig. 4.1b, Video 11). However, this flow configuration induces significant changes in the acoustic wave amplitude (Table 1). We theoretically analyze whether cavitation could occur under these conditions. At 18°C , the saturated vapor pressure of water is $P_v = 2.06\text{KPa}$, the density is $\rho \approx 10^3\text{kg/m}^3$, and the standard atmospheric pressure $P_\infty = 101.33\text{KPa}$. Using the Bernoulli equation, we evaluate the pressure drop at the nozzle exit:

$$P_\infty \approx P_v + \frac{1}{2}\rho V_c^2, \quad (4.1)$$

the critical flow velocity required to induce cavitation is calculated as follows:

$$V_c = \sqrt{\frac{2(P_\infty - P_v)}{\rho}} \approx 14.09\text{m/s}. \quad (4.2)$$

We estimate the mean velocity of the water ejected by the pump. By connecting a flowmeter to the pump, the measured flow rate during operation is approximately $Q =$

7.2 L/min. The mean velocity from the nozzle can be calculated using the continuity equation:

$$v_1 = \frac{4Q}{\pi D_0^2} \approx 3.12 \text{m/s}, \quad (4.3)$$

far below the critical velocity for cavitation.

For a gravity-driven flow setup (Figure 2.3b), no visible bubbles are observed at the pipe outlet after opening the valve. Based on the rate of decline of the water tank's height, the calculated flow rate is approximately $Q_2 = 7.0$ L/min. For the pipe diameter $D_2 = 1.7$ cm shown in Figure 3.2, the average flow velocity inside the pipe is:

$$v_2 = \frac{4Q_2}{\pi D_2^2} \approx 0.51 \text{m/s}, \quad (4.4)$$

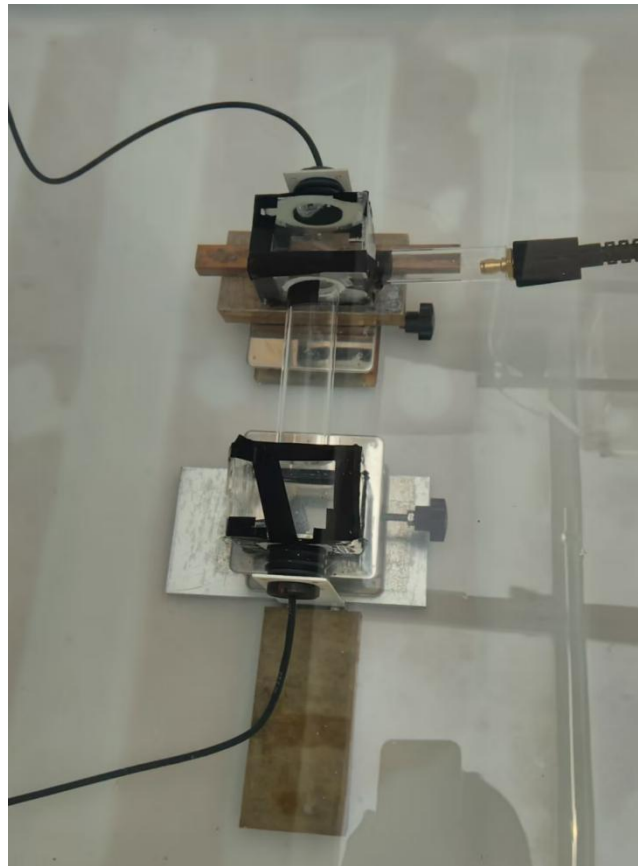
which is also below the critical velocity for cavitation. Therefore, bubble-induced effects can be ruled out in this experiment.

4.2 Resonance

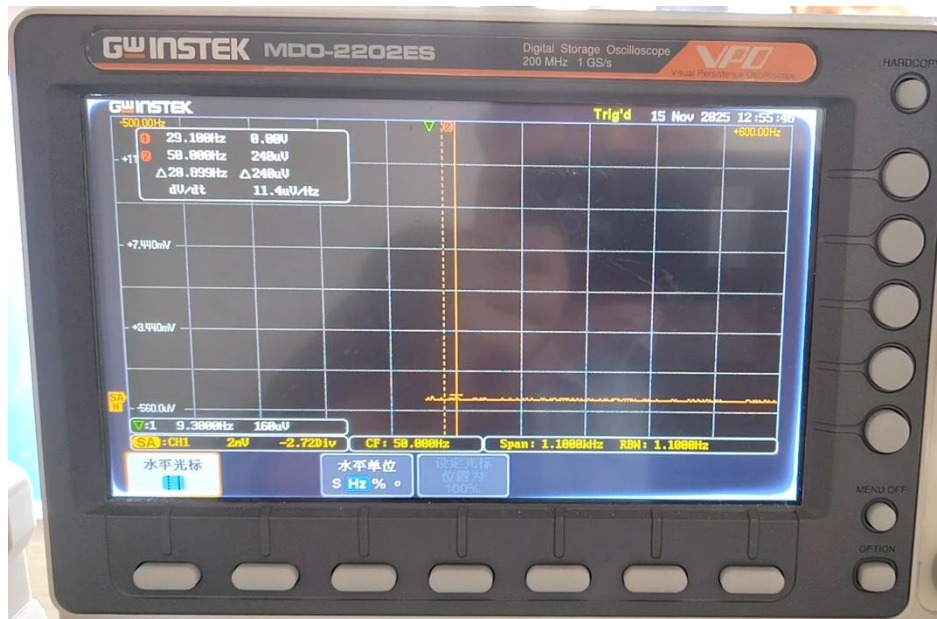
Howe [11] noted that acoustic wave attenuation primarily occurs when the timescales of the sound waves and turbulence are comparable, i.e., a resonance mechanism. Can the observed acoustic variations be attributed to this mechanism? To address this, we conduct measurements and calculations of the fluctuation frequencies generated by turbulence.

First, we measure the frequency spectrum of turbulent fluctuations. The hydroacoustic transducer used in this experiment has a primary frequency of 7 kHz, but it can also detect low-frequency acoustic waves (below 1kHz). In Figure 4.2 and Video 12, we present the receiver spectrum when no acoustic signal is actively

transmitted. Without turbulence (Figure 4.2b), only a slight peak of 0.24 mV is observed at 50 Hz, corresponding to the AC power frequency of the oscilloscope. With turbulence (Figure 4.2c), the 50 Hz peak increased to 0.32 mV (likely due to the 50 Hz AC power input driving the water pump). Additional low-frequency peaks emerged below 50 Hz (e.g., a 29.1 Hz peak of 0.48 mV). When the jet nozzle is moved away from the pipe inlet (disrupting turbulence generation), these spectral peaks disappear. So we can confirm that the turbulent spectrum is concentrated within the 0-50 Hz range.



(a)



(b)



(c)

Figure 4.2 Experiment with the transducer's primary frequency at 7 kHz: (a) experimental setup; (b) receiver spectrum without turbulence; (c) with turbulence. No acoustic signal is actively transmitted.

Next, we theoretically estimate the frequency of turbulent flow. In the setup shown in Figure 4.2, the pipe diameter $D_1=3\text{cm}$. The characteristic velocity can be estimated as $U_1 = Q/A \approx 16.98\text{cm/s}$, where $A = \frac{1}{4}\pi D_1^2$ is the cross-sectional area of the pipe. At room temperature, the kinematic viscosity of water $\nu \approx 10^{-6}\text{m}^2/\text{s}$. The Reynolds number of the flow is $Re = U_1 D_1 / \nu \approx 5094$, and since the incoming flow at the pipe inlet is already turbulent, the flow within the pipe can be assumed to be fully developed turbulence.

First, we examine the dissipation range, characterized by the Kolmogorov scale.

Step 1: Estimating the Friction Velocity

The friction velocity u_* can be derived from the mean flow velocity U_1 and the Darcy-Weisbach friction factor λ . For smooth-pipe turbulence, a widely used approximation is the Blasius formula (see Eq. 20.5 in Schlichting & Gersten [16]):

$$\lambda \approx 0.3164 \cdot Re^{-0.25}. \quad (4.5)$$

Substituting $Re = 5094$, we obtain $\lambda \approx 0.03745$. Then, according to the wall shear stress formula (Eq. 19.24) and (20.4) in Schlichting & Gersten [16]:

$$\tau_1 = \rho(u_*)^2, \quad (4.6)$$

$$\tau_1 = \frac{1}{8} \lambda \rho U_1^2, \quad (4.7)$$

so

$$u_* = U_1 \sqrt{\frac{\lambda}{8}} \approx 1.162\text{cm/s}. \quad (4.8)$$

Step 2: Calculate the energy dissipation rate

In fully developed pipe turbulence, the energy dissipation rate ε can be estimated through global energy balance. For a pipe segment of length L , the power input by the pressure difference ΔP balances the turbulent dissipation power:

$$\dot{W} = \Delta P \cdot Q = \varepsilon LA\rho. \quad (4.9)$$

Furthermore, based on force balance,

$$\Delta P \cdot A = \tau_1 \pi D_1 L. \quad (4.10)$$

Thus,

$$\varepsilon = \frac{4\tau_1 U_1}{\rho D_1} = \frac{4U_1 (u_*')^2}{D_1}. \quad (4.11)$$

Substituting all values, we obtain $\varepsilon \approx 3.056 \times 10^{-3} \text{ m}^2 / \text{s}^3$.

Step 3: Calculate the Kolmogorov scale η

This defines the characteristic size of the smallest eddies, whose energy is dissipated through viscous effects. Its formula is [17]:

$$\eta \approx (\nu^3 / \varepsilon)^{\frac{1}{4}}, \quad (4.12)$$

Substituting all values, we obtain $\eta \approx 1.345 \times 10^{-4} \text{ m}$. The characteristic velocity, time and frequency are

$$v_\eta \approx (\varepsilon \nu)^{\frac{1}{4}}, \quad (4.13)$$

$$t_\eta \approx \sqrt{\frac{\nu}{\varepsilon}} \quad f_\eta = \frac{1}{t_\eta} \approx \sqrt{\frac{\varepsilon}{\nu}}. \quad (4.14)$$

Substituting all values, we obtain $v_\eta \approx 0.7435 \text{ cm/s}$, $f_\eta \approx 55.28 \text{ Hz}$.

For the frequency in the energy-containing range, we take the characteristic length as the pipe radius and the characteristic velocity as the friction velocity or the mean flow velocity, resulting in the large-eddy turnover frequency.

$$f_{L1} = \frac{u_*}{D_1/2}, \quad (4.15)$$

and the flow-through frequency

$$f_{L2} = \frac{U_1}{D_1/2}, \quad (4.16)$$

Substituting all values, we obtain $f_{L1} \approx 0.7747\text{Hz}$, $f_{L2} \approx 11.32\text{Hz}$.

The frequency of the inertial subrange lies between the energy-containing range and the dissipation range. Therefore, the experimentally measured turbulent fluctuation frequency range of 0~50 Hz aligns with the theoretical estimate of 0.78~55 Hz in magnitude. Although there are slight differences in pipe dimensions between Section 3 and Figure 4.2, such as the pipe diameter $D_2=1.7\text{cm}$ in Figure 3.2, $D_3=7.5\text{cm}$ in Figure 3.7 and $D_1=3\text{cm}$ in Figure 4.2, we can reasonably expect that the turbulence frequency magnitudes are similar to the measured values, far below the 60 kHz~4.4 MHz of the acoustic waves generated by the signal generator.

Consequently, turbulent noise cannot resonate with the emitted acoustic waves, failing to satisfy the sound absorption condition described in Howe's theory.

4.3 Viscous Dissipation

Theoretical studies indicate that the amplitude of acoustic signals inside a pipe decays axially along the pipe due to viscous effects in the form of $\exp(-\alpha z)$, where z is the axial distance and α is the attenuation coefficient of the acoustic wave. Howe [11] derived the attenuation coefficient for acoustic waves in a pipe with a stationary fluid:

$$\alpha_0 = \frac{l_A}{2AC} \sqrt{\frac{\omega}{2}} \left[\sqrt{\nu} + (\gamma - 1) \sqrt{\chi} \right], \quad (4.17)$$

where l_A is the pipe perimeter, C is the wave speed, ω is the angular frequency of the signal, γ is the ratio of specific heats, and χ is the thermal diffusivity.

For water at room temperature, we have $C \approx 1500 \text{ m/s}$, $\gamma \approx 1.000 \sim 1.015$ and $\chi \approx 1.43 \times 10^{-7} \text{ m}^2/\text{s}$. In the experiment shown in Figure 3.2, the pipe diameter $D_2 = 1.7 \text{ cm}$, $\omega \approx 2\pi \times 10^6 \text{ Hz}$. Substituting these values into Equation (4.17) yields:

$$\alpha_0 \approx \frac{1}{D_2 C} \sqrt{2\omega\chi} \approx 0.139/\text{m}. \quad (4.18)$$

The Mach number for the flow is

$$Ma = v_2 / C \approx 3.3 \times 10^{-4}. \quad (4.19)$$

In such condition, it has

$$\alpha_i / \alpha_0 \rightarrow 1, (i = 1, 2) \quad (4.20)$$

where α_1, α_2 are the attenuation coefficients when the acoustic wave propagates in the same and opposite directions as the mean flow, respectively [11].

In the pipe experiment conducted by Ronneberger & Ahrens [12], the acoustic wave frequency is 7.35 kHz, and the water flow velocity reaches 50 m/s. The former is far lower than the frequency range (60 kHz~4.4 MHz) in our experiments, while the latter is significantly higher than the flow velocities in our study. According to classical theory, our experiments should exhibit stronger viscous dissipation effects, while the variation in the attenuation coefficient should be very small in turbulent flow.

In Figure 3.2, the distance between the two transducers is $S = 32.0 \text{ cm}$. Under turbulent conditions, more than 40% increase in the acoustic signal compared to the calm state is achieved, so

$$\exp(-\alpha_i \cdot S) / \exp(-\alpha_0 \cdot S) \geq 1.4, \quad (4.21)$$

then, $\alpha_i \leq -1.330/\text{m}$. Similarly, to achieve a 25% reduction in the acoustic signal under turbulent conditions relative to the static state, the following condition must be satisfied:

$$\exp(-\alpha_1 \cdot S) / \exp(-\alpha_0 \cdot S) \leq 0.75. \quad (4.22)$$

So $\alpha_i \geq 1.038/\text{m}$. These are in serious contradiction with Howe's theory [11] and the experimental results on attenuation coefficients by Ronneberger & Ahrens [12].

In addition, for acoustic waves in a pipe, viscous dissipation primarily concentrates near the solid wall, while in free jet, such viscous dissipation is significantly reduced. However, we still observed the absorption and amplification of acoustic waves by turbulence in Table 2. Therefore, the variations in the acoustic signals in this experiment are unrelated to viscous dissipation.

4.4 Scattering

Previous literature suggests that when the turbulent flow frequency significantly differs from the acoustic frequency (consistent with our experimental conditions), sound energy is not absorbed by turbulence but rather scattered [11]. A key signature of turbulence-induced acoustic scattering is spectral broadening [8]. However, our experiments never observe this phenomenon (see Figures 3.3 & 3.4, Videos 4 & 5).

We make a comparison of experimental parameters. In the experiment by Korman & Beyer [8], the jet nozzle diameter is 2.54 cm, flow velocity 6.48 m/s, and acoustic frequency 1 MHz. In Figure 3.9, the corresponding parameters are 0.7 cm nozzle diameter, 3.12 m/s flow velocity, and ~1 MHz acoustic frequency. While the acoustic

frequencies are similar in both cases, the flow Reynolds numbers differ by an order of magnitude. In addition, the distance between the turbulent core region and the two transducers is 65 cm in Korman & Beyer [8], while in our experiment, the distance value is 10~16 cm.

In pipe flow, the confinement by pipe walls prevents acoustic energy from scattering to other spatial locations. Therefore, the observed changes in wave amplitude are evidently unrelated to scattering. In free jet flow, measurements at multiple azimuth angles reveals no obvious variation in acoustic signals (Table 2). This confirms the absence of directional scattering, demonstrating that acoustic variation does not originate from scattering mechanisms.

Then we analyze the Doppler shift effect from a theoretical perspective. Consider a monochromatic plane acoustic wave where the sound source, receiver, and medium are all moving in rectilinear motion along the same direction, with velocities U_s , U_o and U_m , respectively. The relationship between the received frequency ω and the emitted frequency ω_0 satisfies [18]:

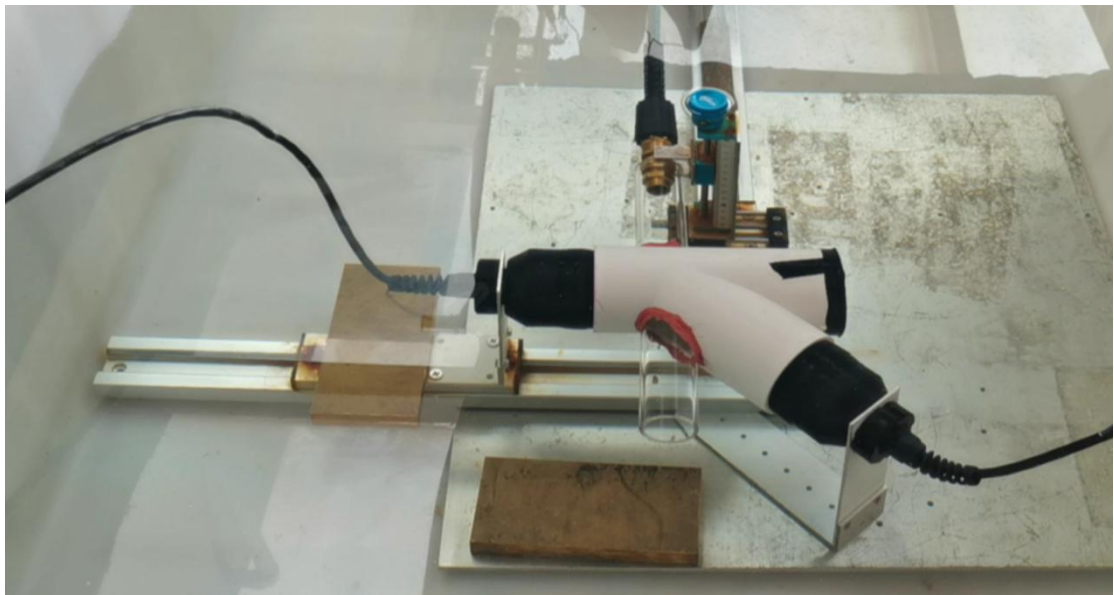
$$\omega = \omega_0 \frac{C + U_m - U_o}{C + U_m - U_s}. \quad (4.23)$$

For the case where the acoustic wave propagates parallel to the mean flow in a pipe, the source and receiver remain stationary $U_s=U_o=0$, while the fluid exhibits a mean axial motion. Under these conditions, $\omega = \omega_0$, no Doppler shift occurs.

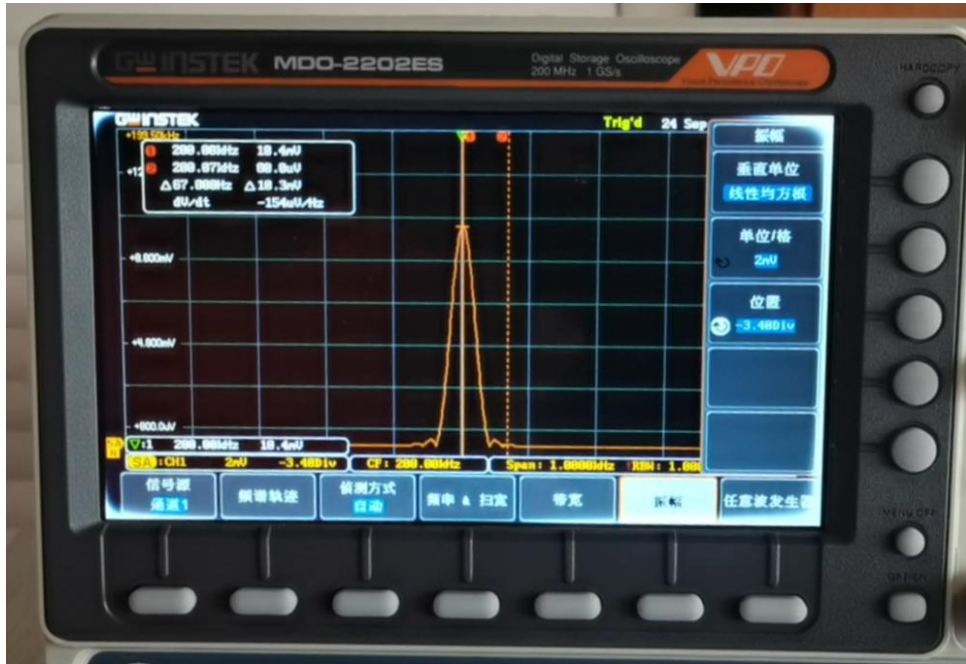
For the case where the acoustic wave propagates perpendicular to the mean turbulent flow, the fluid velocity component in the transverse direction does not affect the acoustic frequency, and thus no Doppler shift occurs. The above theoretical

analysis explains why neither Doppler shift nor spectral broadening is observed in our previous experiments.

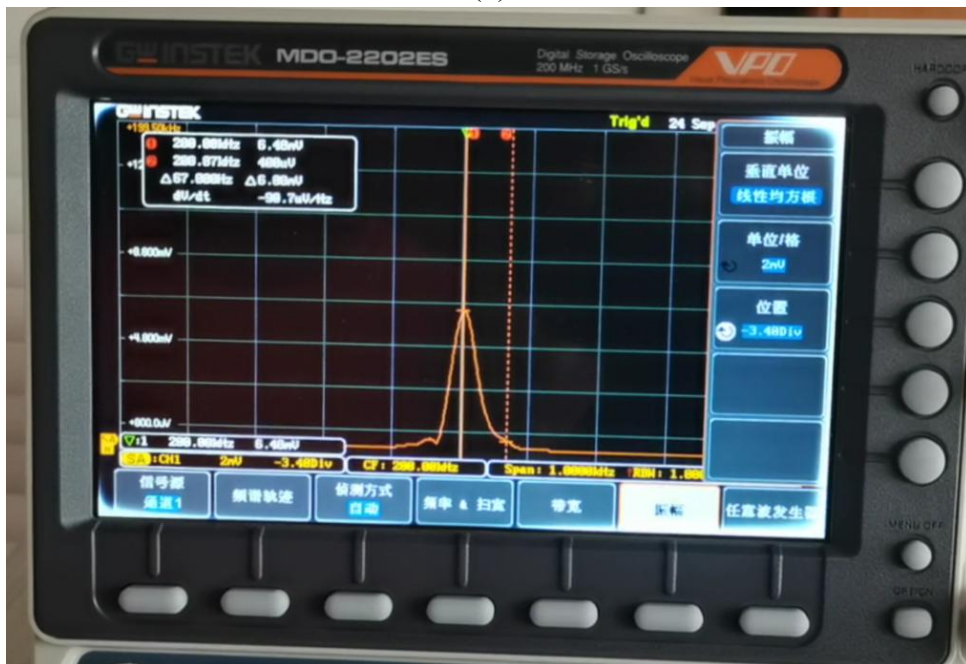
When there is an angle $\theta \neq 0^\circ, 90^\circ$ between the direction of the wave propagation and the direction of fluid motion, a Doppler shift may occur. We position the receiver at an inclination (Figure 4.3), where the left side serves as the transmitter, with its axis perpendicular to the mean flow direction, while the right side functions as the receiver, oriented at a 45° angle to the mean flow direction. Upon the onset of turbulence, the peak amplitude of the received signal decreases, accompanied by a noticeable spectral broadening. These results demonstrate that our instrument is sufficiently sensitive in detecting frequency-based signal variations.



(a)



(b)



(c)

Figure 4.3 Experiment when the receiver is placed at a certain tilt angle: (a) experimental setup; (b) receiver spectrum without turbulence; (c) with turbulence. The signal generator frequency is 200 kHz, and the amplitude is 5 V.

4.5 Mean flow

From the pump-jet and suction experiments in Figures 3.3 and 3.4, we observe that: during suction, the receiver's signal shows no significant difference compared to the static case. A similar result holds when the acoustic waves are perpendicular to the turbulent flow. This indicates that the mean flow motion is not the cause of acoustic variations.

Additionally, in the experiment of Figure 3.2, when the valve is closed to halt the mean flow in the pipe, the receiver signal takes a prolonged period to return to its original stable value under static conditions (Videos 4 & 5). This demonstrates that turbulent fluctuations (even with zero mean velocity) can induce both amplification and attenuation of acoustic signals.

4.6 Temperature

To determine whether the temperature alters the acoustic signal, we measure the temperature near the pipe outlet using thermocouples. In the static case, the water temperature stabilizes at 28.0°C, while turbulent flow results in a minimal increase to just 28.1°C. In a separate controlled experiment with static water, a much larger temperature change from 17.8°C to 18.7°C (0.9°C increase) produces only a minor signal amplitude variation from 21.0 mV to 21.2 mV (a mere 1% change). Given that turbulent flow in the pipe induces temperature fluctuations no greater than 0.1°C—an order of magnitude smaller than the control case—we conclude that temperature effects are negligible and cannot explain the observed variations.

4.7 Mechanical vibration

To what extent do turbulent fluctuation and mechanical vibrations from the acoustic emitter affect the signals receiver? In our experiment, the hydroacoustic transducers are securely wrapped with vibration-damping tape and fixed inside PVC pipes. Both the tape and PVC plastic materials exhibit excellent vibration isolation properties, allowing mechanical vibration interference to be effectively eliminated.

5. Conclusion

This work experimentally examines the effects of turbulence on hydroacoustic wave propagation, focusing on two distinct turbulent flow configurations: pipe flow and free jet. The flows are driven by either a high-pressure pump or hydraulic head difference, with hydroacoustic transducers operating in the 60 kHz to 4.4 MHz frequency range. The results demonstrate that acoustic waves can undergo significant attenuation or amplification when propagating through turbulence, at frequencies far exceeding the characteristic turbulent frequencies. Notably, no spectral broadening is observed in any of the tested conditions.

In pipe flow experiments, both parallel and perpendicular orientations of acoustic waves relative to the mean flow are investigated. Greater signal variation (exceeding 60% in magnitude) occurred in the parallel configuration, suggesting stronger turbulence-wave interaction. For the cases where acoustic waves propagate either in the same direction as or opposite to the mean flow, both scenarios exhibit identical trends in amplitude variation, though the degree of change differs between them. In most cases, the received acoustic signal exhibits small-amplitude oscillations around its mean value when propagating through turbulence. However, under specific

conditions, more pronounced signal oscillations are observed, where instances of both amplitude enhancement and reduction relative to the quiescent state alternately occur. This phenomenon clearly demonstrates that turbulence simultaneously exerts both absorbing and amplifying effects on acoustic wave propagation.

In addition, the total amplification factor of acoustic waves in the entire pipeline is equal to the product of the amplification factors of acoustic waves in each section of the pipeline. At relatively low input voltages, the amplification factor is independent of the input voltage.

When suction is applied near the pipe outlet to induce flow inside the pipe, no variation in received signals is observed. This confirms that laminar flow produces no measurable alteration of acoustic signals. The primary mechanism for acoustic amplitude modulation stems from turbulent fluctuations rather than mean flow. After closing the flow control valve, the mean flow motion ceases, the receiver signal exhibits a finite relaxation period before recovering to its stationary-state value, suggesting the gradually decaying turbulence in the pipeline can still affect the acoustic wave.

For jet-induced turbulence, we investigate the scenario where the acoustic wave propagates perpendicular to the flow direction. The hydroacoustic transducer operated at a frequency of ~ 1 MHz, producing a highly directional sound beam—signal amplitude dropped sharply when the receiver is misaligned by more than 15° . Upon jet activation, the received signal also exhibit amplification or attenuation, while the modulation magnitude is smaller than that in pipe-flow configurations. No significant

signal variation is observed when the receiver is repositioned at different azimuth angles. This confirms that turbulent scattering is not the dominant mechanism for acoustic variation.

For each scenario in this experiment, the amplitude of acoustic waves across all frequency bands either uniformly decreases or increases under the influence of turbulence. There are no instances where some frequency bands decrease while others increase simultaneously, and no new spectral component appears. When the wave propagation direction is parallel or perpendicular to the mean flow, no spectral broadening or Doppler shift are observed. When the transmitter signal is turned off, the receiver no longer detects any signal—regardless of whether the water is stationary, in laminar flow, or turbulent—except for the turbulence-induced frequency. These findings indicate that turbulence only absorbs or amplifies the incident acoustic wave but does not generate new frequency components.

The observed experimental phenomena cannot be explained by conventional mechanisms such as resonance, scattering, or viscous dissipation. This suggests the existence of a previously unknown interaction mechanism between turbulence and acoustic waves. The closest known analogy to our experimental observations is the stimulated absorption and stimulated emission of light, where atoms similarly absorb or amplify incident optical signals. Further research is required to elucidate the physical mechanism underlying turbulence-induced absorption and amplification of acoustic waves.

Appendix

Here, we list the key materials and instruments used in the experiments described in this paper. Figure S.1 displays five types of hydroacoustic transducers, Figure S.2 shows the turbine flowmeter, Table 4 summarizes other major instruments, and Table 5 provides the parameters annotated in the Figures 2.1, 2.2.

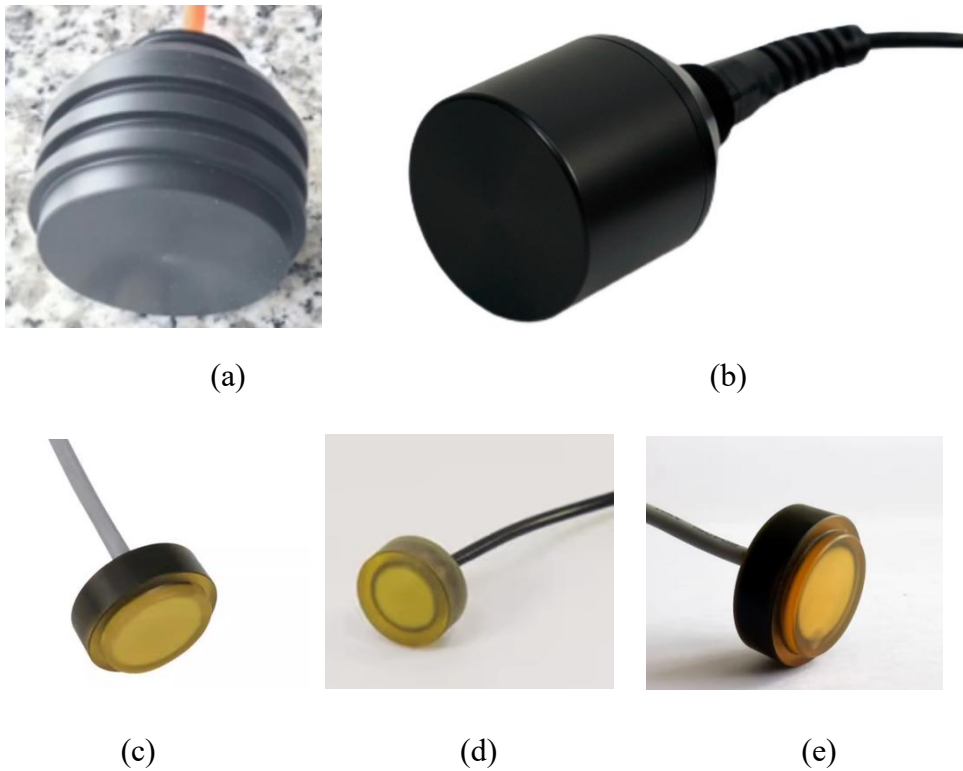


Figure S.1 Hydroacoustic transducers with fundamental frequencies of: (a)7kHz; (b)200kHz; (c)1MHz; (d)2MHz; (e)4MHz. Their outer diameters are 39 mm, 63 mm, 21 mm, 20 mm, and 21 mm, respectively.



Figure S.2 Turbine flowmeter.

Table 4 Instruments

Instrument name	Model	Manufacturer
Signal Generator	2040H	Victor
Oscilloscope	MDO-2202ES	GW Instek
High-pressure pump	—	Zengyuan Electromechanical
	DYW-LS-03A	
	DYW-1M-01	
Hydroacoustic transducer	DYW-4M	Liyu Ultrasonic Technology
	ZDYW-40/200-NA	
	DYW-7-ND	
Manual Linear Stage	40A-35	Hengyu Laser Equipment
Turbine flowmeter	—	Haihui Trading
PVC Fittings	—	Baisheng Pipeline
PVC Pipes	—	Huide Plastic

Table 5 The parameters in Figures 2.1, 2.2

No.	Flow	Transducer's fundamental frequency/MHz	Parameters
1	Pipe flow	1,2,4	$S=32\text{cm}, D=1.7\text{cm},$
2	Pipe flow	0.2	$S=40\text{cm}, D=7.5\text{cm},$
3	Pipe flow	0.007	$S=23\text{cm}, D=3.0\text{cm},$
4	Free jet	1	$h_1=h_3=10\text{cm}, h_2=16\text{cm}$

Data availability

The authors declare that the data supporting the findings of this study are available within the paper and its supplementary information files. Source data are available upon reasonable request.

Declaration of Interests

The authors declare no competing interests.

Author contributions

Kai-Xin Hu made substantial contributions to the conception of the work, wrote the paper for important intellectual content and approved the final version to be published. He is accountable for all aspects of the work in ensuring that questions related to the accuracy or integrity of any part of the work are appropriately investigated and resolved. Yue-Jin Hu designed and fabricated the experimental apparatus, and conducted experimental measurements jointly with Kai-Xin Hu.

Acknowledgments

This work has been supported by the National Natural Science Foundation of China (No.12372247), Zhejiang Provincial Natural Science Foundation (No.LZ25A020009), Ningbo Municipality Key Research and Development Program (No. 2022Z213) and the China Manned Space Engineering Application Program — China Space Station Experiment Project (No. TGMTYY1401S).

References

- [1] Lighthill, M.J., (1952). On sound generated aerodynamically I. General theory. Proceedings of the Royal Society of London. Series A. Mathematical and Physical Sciences, 211(1107), 564-587.
- [2] Lighthill, M. J. (1953). On the energy scattered from the interaction of turbulence with sound or shock waves. Mathematical Proceedings of the Cambridge Philosophical Society, 49(3), 531-551.
- [3] Kraichnan, R. H. (1953). The scattering of sound in a turbulent medium. The Journal of the Acoustical Society of America, 25(6), 1096-1104.
- [4] Baerg, W., & Schwarz, W. H. (1966). Measurements of the scattering of sound from turbulence. The Journal of the Acoustical Society of America, 39(6), 1125-1132.
- [5] Brown, E. H., & Clifford, S. F. (1976). On the attenuation of sound by turbulence. The Journal of the Acoustical Society of America, 60(4), 788-794.
- [6] Campos, L. M. B. C. (1978). The spectral broadening of sound by turbulent shear layers. Part 1. The transmission of sound through turbulent shear layers. Journal

of Fluid Mechanics, 89(4), 723-749.

- [7] Campos, L. M. B. C. (1978). The spectral broadening of sound by turbulent shear layers. Part 2. The spectral broadening of sound and aircraft noise. *Journal of Fluid Mechanics*, 89(4), 751-783.
- [8] Korman, M. S., & Beyer, R. T. (1980). The scattering of sound by turbulence in water. *The Journal of the Acoustical Society of America*, 67(6), 1980-1987.
- [9] Korman, M. S., & Beyer, R. T. (1988). Nonlinear scattering of crossed ultrasonic beams in the presence of turbulence in water. I: Experiment. *The Journal of the Acoustical Society of America*, 84(1), 339-349.
- [10] Ingard, U., & Singhal, V. K. (1974). Sound attenuation in turbulent pipe flow. *The Journal of the Acoustical Society of America*, 55(3), 535-538.
- [11] Howe, M. S. (1984). On the absorption of sound by turbulence and other hydrodynamic flows. *IMA Journal of Applied Mathematics*, 32(1-3), 187-209.
- [12] Ronneberger, D., & Ahrens, C. D. (1977). Wall shear stress caused by small amplitude perturbations of turbulent boundary-layer flow: an experimental investigation. *Journal of Fluid Mechanics*, 83(3), 433-464.
- [13] Peters, M. C. A. M., Hirschberg, A., Reijnen, A. J., & Wijnands, A. P. J. (1993). Damping and reflection coefficient measurements for an open pipe at low Mach and low Helmholtz numbers. *Journal of Fluid Mechanics*, 256, 499-534.
- [14] Weng, C., Boij, S., & Hanifi, A. (2015). On the calculation of the complex wavenumber of plane waves in rigid-walled low-Mach-number turbulent pipe flows. *Journal of Sound and Vibration*, 354, 132-153.

- [15] Weng, C., Boij, S., & Hanifi, A. (2013). The attenuation of sound by turbulence in internal flows. *The Journal of the Acoustical Society of America*, 133(6), 3764-3776.
- [16] Schlichting, H., & Gersten, K. (2016). *Boundary-layer theory*. Springer.
- [17] Pope, S. B. (2000). *Turbulent flows*. Cambridge university press.
- [18] Pierce, Allan D. (2019). *Acoustics: an introduction to its physical principles and applications*. Springer.